

Earthquake Design Pressures from Soil Interaction on Building Basement Walls

J.H. Wood

Retired Civil Engineer, Lower Hutt, New Zealand.

ABSTRACT

Free-standing retaining walls are usually designed for earthquake pressures assuming cohesionless soil backfill and using the Mononobe-Okabe method (M-O), (Mononobe & Matsuo, 1929). This method assumes active pressure develops as a consequence of a failure wedge in the backfill soil. Building basement walls are usually relatively stiff or restrained from relative displacement so the active pressure state is unlikely to arise. In addition, two components of dynamic pressure that develop on the wall need to be considered. The first of these is due the shear deformations in the soil generated by the earthquake waves. The second results from the inertia forces of the building above ground level generating movements of the wall against the soil. There is no established design method that considers both of these components.

A number of recent centrifuge and analytical studies consider the loading from the wave generated soil deformations. Previous analytical studies consider buildings founded on rock or very stiff soil but these are not typical foundations of many buildings with basements that are founded on piles or a raft foundation.

The paper reviews some of the published research on earthquake pressures on basement walls. Results are presented from elastic finite element analyses (FEA's) undertaken as part of the present study and calibrated against experimental results. Because of the wide range of building geometries and foundation types it is not possible to develop a simple empirical method that is widely applicable. Instead, it is concluded that simplified elastic FEA should be part of the design process to estimate the earthquake induced pressures.

1 INTRODUCTION

No significant damage to engineered retaining structures or basement walls was reported in recent major earthquakes including the 2010-11 Canterbury earthquakes, subduction earthquakes in Chile 2010 and Japan, 2011, the 2016 Kumamoto, Japan and the 2017 Puebla, Mexico earthquakes. Satisfactory earthquake performance suggests that basement walls designed for at-rest gravity soil pressures have good resistance to earthquake induced soil pressures.

Extensive research involving both analytical and experimental studies has been carried out on earthquake induced soil pressures on free-standing retaining walls and design procedures are well established (for example the M-O method). In contrast studies on the earthquake induced soil pressures on building basement walls is limited. While recent research has acknowledged that embedded basement walls should be considered in the building seismic design, no specific provisions have been proposed or adopted.

Several of the more frequently referenced methods of determining earthquake induced soil pressures on basement walls are summarised in the following sections.

1.1 Ostadan Method

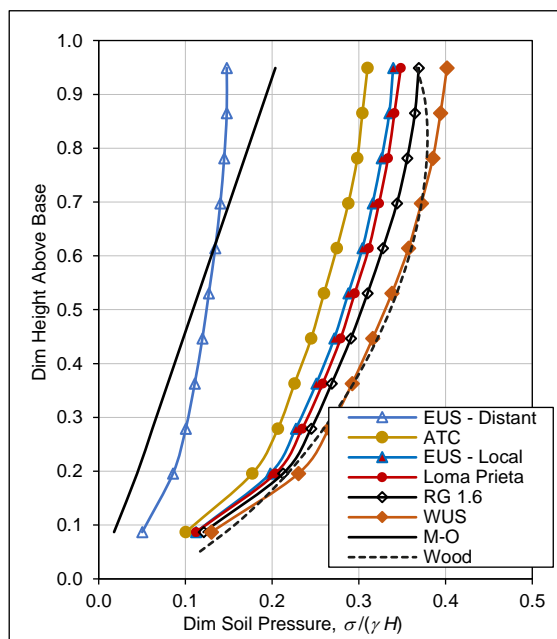


Figure 1. Comparison of earthquake soil pressures. From Ostadan, 2008 (modified).

The method proposed by Ostadan, 2008 to estimate earthquake pressures involves carrying out a one-dimensional soil column analysis (using a program such as SHAKE) to obtain the response in terms of a 30 percent damped acceleration response spectrum at the depth corresponding to the base of the wall in the free-field. An empirical equation is then used to compute the equivalent mass of the soil layer interacting with the wall which is assumed to be a representative SDOF system. The lateral seismic force on the wall is computed from the product of the equivalent mass and the spectral acceleration at the frequency of the soil column at the base of the wall. The maximum lateral seismic soil pressure at the ground surface level is obtained by dividing the lateral force obtained by the area under a normalized seismic soil pressure distribution. The pressure profile is obtained from the peak pressure and an empirical pressure distribution relationship.

Ostadan compared earthquake soil pressures from his method with the M-O, and the rigid wall method of Wood, 1973 for a 9.2 m high basement wall embedded in soil with a shear wave velocity of 305 m/s. All the ground motions were scaled to 0.30 g peak ground acceleration (PGA). For the M-O method, it was assumed that the earthquake soil pressure had an inverted triangular distribution. The M-O method and the Wood rigid wall assumption generally result in the lowest and maximum pressures respectively. The Ostadan method gives a range of pressure profiles, depending on the frequency content of the input motion. Figure 1 shows the comparison presented by Ostadan.

1.2 British Columbia

Taiebat et al, 2014 report a major study on the behaviour of basement walls during earthquakes. A typical four-storey basement wall structure was designed for different fractions of the design level PGA of 0.45 g for Vancouver (2% probability in 50 years). Dynamic nonlinear soil–structure interaction analyses were conducted on numerical models of the walls accounting for their flexibility and yield moments. The model was subjected to seven ground motions matched to the ultimate hazard spectrum. Pressures, bending moments, shear forces, lateral deformations, and drift ratios over the height of the walls were presented. The drift ratios were a measure of yield deformation from plastic hinge rotations in the walls and a 2% drift ratio was considered acceptable. The sensitivity of the results to variations in the soil constitutive model was evaluated. It was concluded that basement walls founded on dense soil can be designed using the M–O method with an inverted pressure distribution, but with an acceleration of 50%–60% PGA instead of 100%.

1.3 Centrifuge Tests

A number of centrifuge tests have been carried out on 1/36 scale model walls that represent both basement and stiff wall structures. The scale of the models allowed the structures to be founded on soil instead of being mounted directly on a rigid base as has been the case in most shaking table tests. Experiments reported

by Mikola & Sitar, 2013 and Candia & Sitar, 2013 modelled fixed base free standing cantilever structures retaining cohesionless and cohesive soils. All of the walls were 6.5 m high in prototype scale and were founded on a 13.5 m deep soil layer. An experiment by Wagner & Sitar, 2016 modelled a 13.3 m deep braced basement type wall structure retaining cohesionless soil and was founded on a 6.7 m deep soil layer. The geometry of the structure and the extent of the soil backfill and founding soil layer is shown schematically in Figure 2. The soil layer and backfill are drawn approximately to scale.

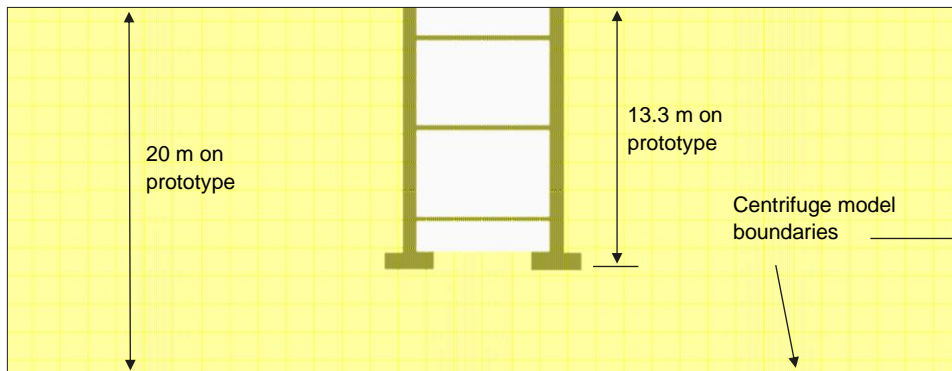


Figure 2. 13.3 m deep model basement wall structure studied by Wagner & Sitar, 2016.

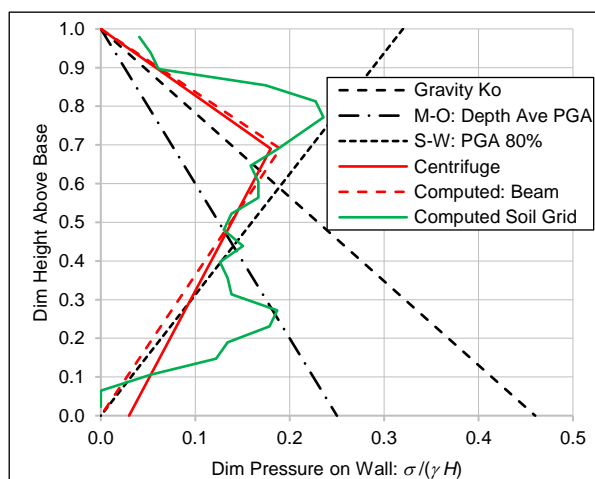


Figure 3. Pressure comparisons – computed and centrifuge for acceleration time-history. From Wagner & Sitar, 2016 (modified).

Wagner & Sitar also carried out numerical studies using the FLAC (Itasca, 2012) software to simulate the centrifuge study of the 13.3 m deep basement model. Numerical work was extended to include basements with three 8 m wide bays and overall depths of 3, 6, 9 and 12 m.

The dynamic earth pressure in the centrifuge experiment was estimated by removing the wall inertia loads (using recorded accelerations) from forces measured by load cell installed in the bracing beams between the wall members and distributing the adjusted forces using tributary areas. The soil pressures on the walls in the numerical simulation were interpreted from both the axial loads in the bracing beams and the dynamic earth pressures in the soil mesh adjacent to the wall members. Typical experimental and numerical dynamic earth

pressure distributions corresponding to the maximum dynamic force pressure increment are shown in Figure 3 for one of acceleration time-history input motions. The experimental and numerical results are compared with the M-O and the Seed and Whitman, 1970 (S-W) pressure distributions. The S-W method is based on M-O but with the centre of pressure at 0.6 of the wall height from the base. The M-O distribution was computed using the maximum averaged acceleration over the depth of embedment of the basement. The S-W, dynamic earth pressure distribution was computed using 80% of the PGA at the ground surface.

The Wagner & Sitar 13.3 m deep basement structure was investigated in the present study using an elastic FEA model. This indicated that because of rotations of the wall footings the basement structure was more flexible than many basement structures that are usually stiffened by end walls and intermediate dividing walls and frames. Estimating the dynamic soil pressures from the load cells in the bracing beams may have led to an underestimation of the dynamic pressures because if the soil stiffness is equal on either wall, the displacements in the first mode response of the soil layer are symmetrical about the structure centreline and

for this case the theoretical axial loads in the bracing beams are zero. Higher modes of the soil layer will induce axial loads in the bracing but the first mode is likely to have the largest response. Also, the soil stiffness will vary to some extent between the wall faces as at any instance of time one will have a tension dynamic pressure component and the other a corresponding compression component. On the tension side soil gapping will develop over the top part of the wall where the gravity static pressures are low. The elastic FEA indicated that the inertia loads from the walls increased the soil pressures so making deductions to bracing loads for wall inertia effects may also have introduced error.

1.4 Hushmand Reservoir Study

Hushmand, 2016 carried out a series of sixteen centrifuge model experiments on 10 to 12 m high reinforced concrete underground reservoir structures. The structures were buried in either a dry medium-dense sand or a silty sand with different slopes on the backfill surface. A suit of earthquake ground and sinusoidal motions were applied to the models. The structure stiffness, backfill soil type, surface slope, embedment depth, and input ground motion characteristics were varied to evaluate their influence on structural performance. Two-dimensional 1/60 scale models were constructed to match the mass, lateral stiffness, and natural frequency of typical prototype reservoir structures. The structural stiffness was varied by changing the thickness of the walls, roofs and base slabs and keeping the height, width, and length the same. The models were fabricated from welded steel plates to give moment connection at the corners. The stiffness of the two stiffest models was reasonably typical of basement structures of similar height.

Soil pressures against the walls were measured using tactile sensors mounted on the surface of the model walls. The experimental results are of particular interest because the soil pressures were measured directly and this does not appear to have been done successfully in other reported experimental studies.

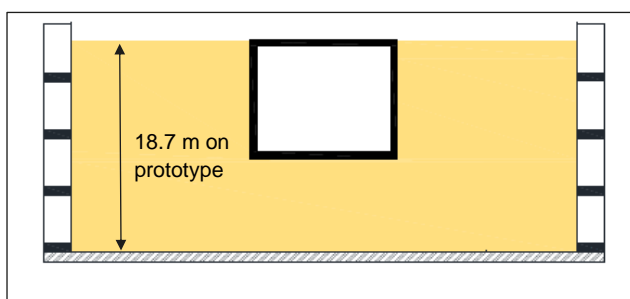


*Figure 4. Schematic of centrifuge models with ground surface at roof level.
From Hushmand, 2016,*

Three of the tests were carried out using cohesionless soil with the reservoir roof at the surface of level ground (similar to a basement wall). A schematic layout of the centrifuge model and soil layer used in these tests is shown in Figure 4.

A triangular distribution of dynamic pressure similar to the conventional M-O distribution (maximum pressure at the wall base) was measured on the most flexible structure, A more uniform pressure distribution with higher pressures was measured on the two stiffer structures. (See Figure 8 below.)

1.5 Li and Aguilar

Li and Aguilar, 2000 estimated earthquake induced soil pressures on a rigid wall supported on an elastic foundation using an analytical elastic dynamic method. Both the foundation and backfill were viscoelastic; the foundation was a semi-infinite half-space and the backfill a uniform layer of constant thickness. The wall was assumed to rotate on the elastic foundation but was restrained from horizontal displacement. The wall-backfill schematic is shown in Figure 5. The analytical solution was developed by assuming an approximate backfill-foundation interface condition and adopting the least squares method.

The transient response of the system was studied by obtaining spectra for base shear. A large number of seismic records were analysed to obtain average spectra and three correction functions were used to take into account the foundation stiffness and density, and the wall inertia.

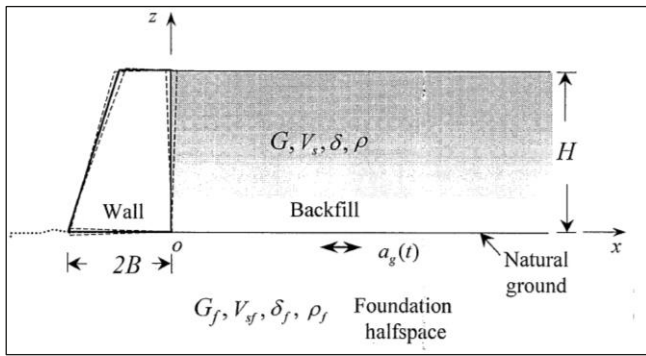


Figure 5. Wall-backfill-foundation system.
From Li and Aguilar, 2000.

Results were presented for the static (low frequency forcing) base shear on a wall with a ratio of the base width to height of 0.4 and for various ratios of the wall mass per unit area to the backfill density. The analytical expressions are not straightforward to evaluate so the results are not directly applicable to basement walls if their geometry differs significantly from the width to height ratio of 0.4. The results show that when the wall is supported on a deep foundation with similar elastic properties to the backfill layer the static base shear is reduced by a factor of approximately 0.5 from the rigid foundation case.

A simple design method to estimate the maximum base shear was presented. The method is more applicable to practical application than similar earlier work undertaken by Veletsos and Younan, 1997 and Younan and Veletsos, 2000 on the earthquake response of flexible walls supporting a uniform elastic backfill.

2 ELASTIC FEA STUDY

The review of published research on earthquake pressures on basement walls showed that the commonly accepted and recently proposed methods gave very large variations in the earthquake dynamic pressure component. The Ostadan, 2008 method typically gave pressures approaching those expected on rigid walls located on a stiff foundation whilst the Taiebat et al, 2014 pressures based on reduced M-O pressures were much lower. Some of the centrifuge results also gave unexpectedly low pressures although the direct dynamic pressure measurements made by Hushmand, 2016 on model reservoir structures with similar stiffness to typical basement walls were higher than indicated by other tests. To explore these differences a study using a simple elastic FEA method was instigated. Initially the models used in the centrifuge tests were investigated. The work was extended to other basement geometries and finally the influence of a typical concrete framed building superstructure supported on a foundation basement of moderate depth was considered. Some of the results of the present study are summarised in the following sections.

2.1 Centrifuge Tests of Wagner & Sitar

The 13.3 m deep centrifuge model basement investigated by Wagner and Sitar was analysed using the elastic FEA method. The schematic of the model is shown in Figure 2. A uniform fine mesh of 0.1 x 0.1 m was used for both the structure and walls. This was easy to generate and results in modest compute times. Both static analyses using a uniform horizontal body force and dynamic modal analyses were carried out.

The walls of the model were 0.47 m thick in prototype scale and constructed of aluminium alloy. They were stiffened with vertical ribs and in the two-dimensional FEA model assumed to have a uniform thickness of 0.7 m to give a similar moment of inertia of the walls to the model. The wall footings were 2.7 m wide and 0.9 m deep. Soil boundaries at the left and right of the model were assumed restrained in the vertical and free in the horizontal directions. The soil in the elastic FEA was assumed to be uniform over the height of the model and founding soil with a Young's modulus, E of 50 MPa and a Poisson's ratio, ν of 0.33. Soil pressures on the wall are not sensitive to these values but are affected by any vertical variation in the elastic constants. Under the 0.5 g earthquake load used in the analysis (uniform body force for the static analysis and free field on the ground surface in the dynamic analysis) tension pressures occur near the top of the walls. A gap of depth 1.8 m was assumed to approximately model this effect. Below this depth the gravity soil pressures will prevent significant tension pressures at the wall face.

Paper 28 – Earthquake Design Pressures from Soil Interaction on Building Basement Walls

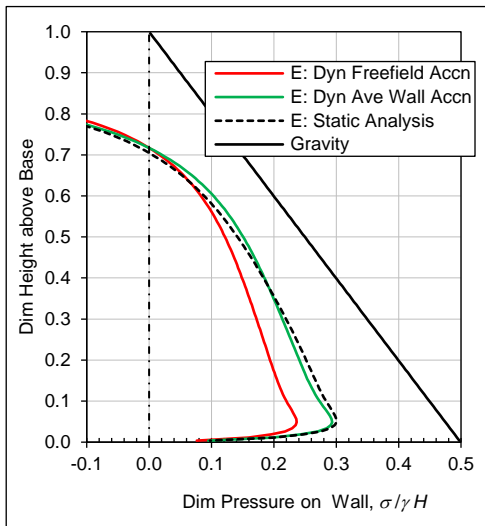


Figure 6. Pressures from elastic FEA.

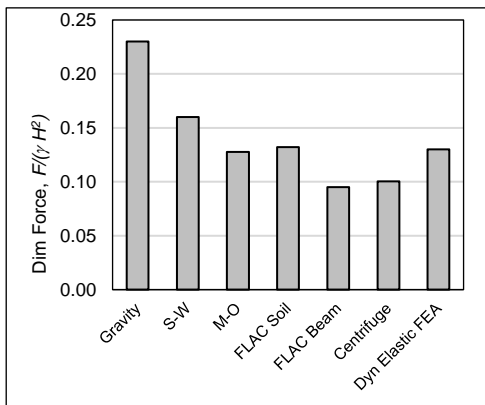


Figure 7. Force components on wall from various analyses methods.

Pressure distributions calculated by the elastic FEA's are shown in Figure 6. The dynamic pressure component was computed using only the first mode response (frequency 1.48 Hz). In one dynamic case the free-field acceleration on the soil surface at the soil end boundaries was used to calculate the response and in the other the average acceleration over the height of the wall. This later procedure gives good agreement with the static analysis based on a uniform 0.5 g body force.

The earthquake pressure components are not similar in shape to the experimental and numerical pressures shown in Figure 3 (reproduced from Wagner & Sitar, 2016; the earthquake input motion had an average ground surface PGA of 0.5 g). The elastic FEA pressures were strongly influenced by rotation of the basement walls about their base and a reason for the difference could be related to the stiffness of the cross beams which affect this rotation. They may have been stiffer in the centrifuge model than assumed in the elastic FEA.

Force components obtained by integrating the pressures shown in Figures 3 and 6 are shown in Figure 7. Although the pressure distributions are not very similar there is reasonable agreement between the earthquake force from the soil mesh pressures in the Wagner and Sitar FLAC analysis and the elastic FEA of the present study. For comparison, the dimensionless earthquake force [$Force/(\gamma H^2)$] from a 0.5 g static body force acceleration acting on a rigid smooth wall supported on a rigid foundation is 0.49 indicating that the Wagner and Sitar basement wall was very flexible (25% of rigid wall force).

2.2 Centrifuge Tests of Hushmand

The intermediate stiffness reservoir model used by Hushmand in his experimental centrifuge study was analysed using the elastic FEA method described in Section 2.1. Figure 4 shows the schematic layout of the centrifuge model and a similar structure-soil layout was used in the FEA. In prototype scale the reservoir thicknesses of the roof, walls and floor were 0.4, 0.6 and 0.7 m respectively. The overall height and widths of the structure were 10.5 and 12.2 m respectively. The depth of the soil layer below the structure was 8.2 m and the distance of the soil end boundaries from either side of the structure 14.9 m. Both a uniform soil with E of 50 MPa and non-uniform soil with this modulus varied from 40 MPa at the surface to 60 MPa at the base were used. The Poisson's ratio for both soil types was taken as 0.33. The soil was assumed to be in bonded contact over the complete height of the walls.

Figure 8 compares the earthquake pressures from one of the centrifuge experiments with the pressures calculated for the first mode response in the elastic FEA using the same free-field ground surface PGA (0.81 g). The FEA results are for the non-uniform soil ($E = 40-60$ MPa) and show good agreement with the experimental pressures over most of the wall height.

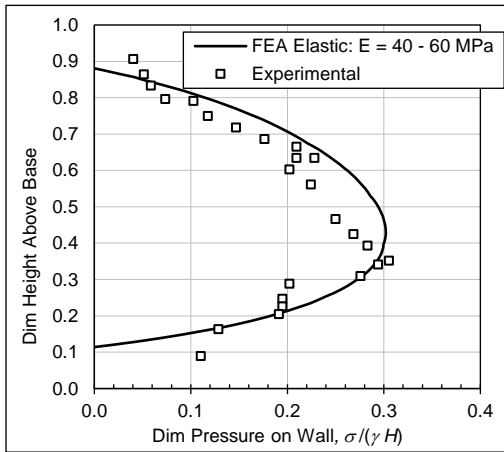


Figure 8. Pressures from Hushmand intermediate stiffness model.

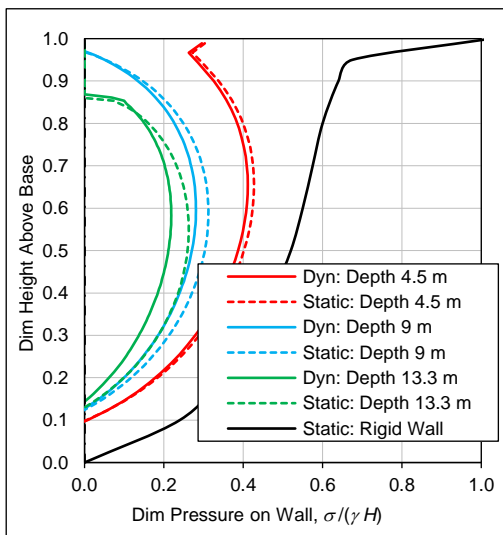


Figure 9. Earthquake pressures on basement walls of various depths.

2.3 Influence of Basement Depth

The elastic FEA method described in Sections 2.1 and 2.2 was used to investigate the influence of the depth of the basement wall on the earthquake soil pressures. Wagner and Sitar, 2016 indicated that this was an important parameter. The overall width of the basement was taken as 9 m, similar to the width of the 13.3 m deep basement used in the Wagner and Sitar experiment. Overall depths of 4.5, 9.0 and 13.3 m were investigated with the overall soil layer depth maintained at 20 m. The basement was assumed to be rigid with a mass density of 0.53 t/m^3 . A uniform soil with E of 50 MPa and ν of 0.33 was used. The soil was in bonded contact with the walls over their complete height.

Earthquake pressures from both the static and dynamic first mode analyses are shown in Figure 9 and are compared with the earthquake pressure on a rigid wall on a rigid foundation (no force from wall inertia). The static analysis results are for a 0.5 g body force and the dynamic results for a 0.5 g free field ground surface acceleration. The basement depth clearly has an influence on the pressures but this was mainly a result of the deeper basements having greater rotation from foundation soil flexibility than the shallow 4.5 m deep basement.

2.4 Building Superstructure

Earthquake forces from a building superstructure will be transferred to any embedded basement and may result in significant translation and rotation deformations of the basement. These deformations will generate pressures against the walls of the basement. Clearly the pressures from superstructure forces can be expected to be greater for tall buildings rather than the case for low-rise structures.

In the present study the effect of a building superstructure on the earthquake induced pressures on a basement was investigated by carrying out the analysis of a typical 10-storey concrete framed building located in the Wellington area. The building had a plan area of 19 x 44 m, a height above ground of 28.3 m, a mass density of 0.23 t/m^3 and a first mode period of 1.5 s for response in the narrow direction. It was assumed to be founded on a basement structure having a depth of 4.5 m and of similar plan dimensions to the superstructure. NZS 1170.5 was used to calculate the design level forces at the interface of the superstructure and basement assuming a ductility factor of 6 and an overstrength factor applied to the superstructure design forces of 1.5. The soil was assumed to be uniform Class D with an E of 50 MPa and an overall depth of 20 m from ground surface to an underlying rigid rock layer. The superstructure unfactored design base shear was calculated to be 3.6 MN and the base overturning moment (OTM) 70 MN m.

A static FEA analysis was carried out on the basement loaded with the superstructure factored design shear force and moment. The analysis also considered separately the response of the soil layer against the basement wall. The applied body force acceleration of 0.45 g was the site PGA calculated from NZS1170.5. The soil was assumed bonded to the basement wall without tension gapping.

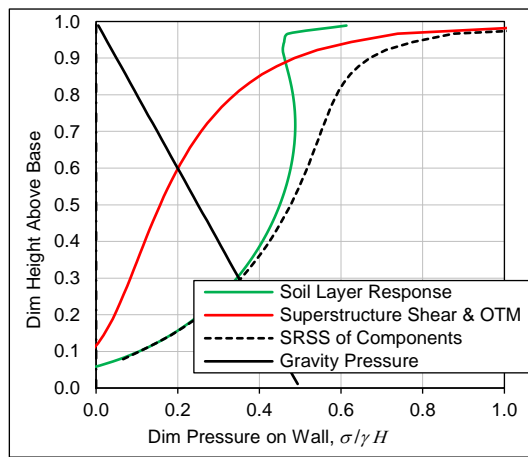


Figure 10. Earthquake pressures on basement with 10-storey superstructure.

Figure 10 shows the earthquake pressure components from the superstructure forces acting on the basement and the soil layer response. The pressure from the soil gravity load is shown for comparison. The first mode of the soil layer response was estimated to have a period of 0.7 s and because this differed significantly from the building period it was considered satisfactory to combine the two earthquake pressure components by the square root of the sum of the squares method (SSRS).

The building superstructure forces result in a significant increase in the pressures on the basement wall over the top section. Most of the increase arises from rotation of the basement under the superstructure OTM and its plan dimensions will clearly affect the amount of rotation.

3 CONCLUSIONS

Recognised analyses methods give a wide variation in earthquake pressures on basement walls. To resolve this issue it is proposed that pressures for design be estimated using simple elastic static or dynamic FEA. Static analyses will give moderately conservative pressures and a refinement is to use the first mode in a simple modal analysis. This approach was checked in the present study by making comparisons with the direct pressure measurements made in centrifuge experiments by Husmand, 2016 and found to be satisfactory. The method can be extended to include the effects of superstructure earthquake forces which may be significant for high-rise buildings.

An elastic FEA basement model with a uniform fine mesh can be set up rapidly in most software packages and will have very modest compute times on modern laptop computers for both static and modal dynamic analyses. A fine mesh enables the geometry of the basement to be accurately modelled and in most cases a single or several two-dimensional models will be satisfactory. There will be uncertainty in the equivalent elastic properties for the soil but provided the variation with depth is reasonably realistic the results will not be very sensitive to the absolute values of the soil properties. An elastic model enables sensitivity analyses to be rapidly carried out using upper and lower bounds for the soil properties to quantify the influence of the soil assumptions on the soil pressures.

There do not appear to be simple empirical analytical methods that can adequately cover the wide range of basement and superstructure configurations and the site soil conditions. Non-linear FEA using time-history acceleration inputs can be used but this adds considerable complexity and may not give more reliable results than a simple static elastic FEA.

REFERENCES

- Candia G and Sitar N (2013). "Seismic Earth Pressures on Retaining Structures in Cohesive Soils". Report No. UCB GT 13-02, August 2013, 161pp.
- Hushmand A, Dashti S, Davis C, Hushmand B, Zhang M, Ghayoomi M, McCartney JS, Lee Y and Hu J (2016). "Seismic performance of underground reservoir structures: Insight from centrifuge modeling on the influence of structure stiffness." *ASCE, Journal of Geotechnical and Geoenvironmental Engineering*, 142(7). [https://doi.org/10.1061/\(ASCE\)GT.1943-5606.0001477](https://doi.org/10.1061/(ASCE)GT.1943-5606.0001477)

- Itasca (2012). “*FLAC: Fast Lagrangian Analysis of Continua, Ver. 7.0*”. Itasca Consulting Group, Inc., Minneapolis. <https://www.itascacg.com/>
- Li X and Aguilar O (2000). “Elastic earth pressures on rigid walls under earthquake loading”. *Journal of Earthquake Engineering*, **4**(4): 415-435. <https://doi.org/10.1080/13632460009350378>
- Mikola RG and Sitar N (2013). “*Seismic Earth Pressures on Retaining Structures in Cohesionless Soils*”. Report No. UCB GT 13-01, March 2013, 217pp.
- Mononobe N and Matsuo H (1929). “On the determination of earth pressure during earthquakes”. *Proceedings of the World Engineering Conference*, **9**: 179-187.
- Ostadan F (2008). “Seismic soil pressure for building walls – an updated approach”. *Bechtel Technology Journal*, **1**(1): 3-12.
- Seed HB and Whitman RV (1970). “Design of earth retaining structures for dynamic loads. *ASCE Specialty Conference, Lateral Stresses in the Ground and Design of Earth Retaining Structures*. Cornell University, Ithaca, New York, 103-147.
- Standards New Zealand (2004). “*NZS1170.5: Structural Design Actions. Part 5: Earthquake Actions - New Zealand*”. Standards New Zealand, Wellington, 76pp. <https://www.standards.govt.nz/sponsored-standards/building-standards/NZS1170-5>
- Taiebat M, Amirzehni E and Finn WDL (2014). “Seismic design of basement walls: evaluation of the current practice in British Columbia”, *Canadian Geotechnical Journal*, **51**(9): 1004-1020. <https://doi.org/10.1139/cgj-2013-0212>
- Veletsos AS and Younan AH (1997). “Dynamic response of cantilever retaining wall”. ASCE, *Journal of Geotechnical and Geoenvironmental Engineering*, **123**(2): 161-172. [https://doi.org/10.1061/\(ASCE\)1090-0241\(1997\)123:2\(161\)](https://doi.org/10.1061/(ASCE)1090-0241(1997)123:2(161))
- Wagner N and Sitar N (2016). “Influence of the depth of embedment on seismic earth pressures on basement walls”. *16th World Conference on Earthquake Engineering (16WCEE)*, 9-13 January 2017, Santiago, Chile, Paper N° 1023, 11pp. <https://www.wcee.nicee.org/wcee/article/16WCEE/WCEE2017-1023.pdf>
- Wood JH (1973). “*Earthquake-Induced Soil Pressures on Structures*”. Report EERL 73-05, Earthquake Engineering Research Laboratory, California Institute of Technology, Pasadena, California. 311pp.
- Younan AH and Veletsos AS (2000). “Dynamic response of flexible retaining walls. *Earthquake Engineering and Structural Dynamics*, **29**: 1815-1844. [https://doi.org/10.1002/1096-9845\(200012\)29:12%3C1815::AID-EQE993%3E3.0.CO;2-Z](https://doi.org/10.1002/1096-9845(200012)29:12%3C1815::AID-EQE993%3E3.0.CO;2-Z)